Molecular beam epitaxy of phase pure cubic InN

J. Schörmann,[a] D. J. As, and K. Lischka
Department Physik, Universität Paderborn, Warburger Strasse 100, 33098 Paderborn, Germany

P. Schley and R. Goldhahn
Institut für Physik, TU Ilmenau, PF 100565, 98684 Ilmenau, Germany

S. F. Li, W. Löffler, M. Hetterich, and H. Kalt
Institut für Angewandte Physik, Universität Karlsruhe, 76128 Karlsruhe, Germany

(Received 28 September 2006; accepted 22 November 2006; published online 26 December 2006)

Cubic InN layers were grown by plasma assisted molecular beam epitaxy on 3*C*-SiC (001) substrates at growth temperatures from 419 to 490 °C. X-ray diffraction investigations show that the layers have zinc blende structure with only a small fraction of wurtzite phase inclusions on the (111) facets of the cubic layer. The full width at half maximum of the *c*-InN (002) x-ray rocking curve is less than 50 arc min. The lattice constant is 5.01±0.01 Å. Low temperature photoluminescence measurements yield a *c*-InN band gap of 0.61 eV. At room temperature the band gap is about 0.56 eV and the free electron concentration is about $n \sim 1.7 \times 10^{19}$ cm^{-3}. © *2006 American Institute of Physics*. [DOI: 10.1063/1.2422913]

Recently, great interest in nonpolar III-nitrides—including cubic III-nitrides—has risen due to the absence of the built-in electrostatic field, which can limit the performance of devices. Within this family of semiconductors InN is the material with the smallest band gap, smallest effective mass, and highest electron mobility.[1,2] Therefore a great potential of application in electronic and optoelectronic devices of pure InN is expected. However, up to now the crystal quality of InN epilayers led to a strong and controversial debate of even fundamental parameters such as the band gap energy.[3] The development and improvement of InN growth techniques led to a reexamination of the band gap and evidenced a narrow fundamental band gap of hexagonal InN of about 0.9 (Ref. 4) or between 0.6 and 0.7 eV.[5–7] For cubic InN (*c*-InN) an even lower band gap energy of around 0.58 eV is expected,[8] which would expand the applications of group III-nitrides towards the infrared range. However, the cubic III-nitride polytype is metastable and can only be grown in a narrow window of process conditions.[9,10] Under nonoptimum growth conditions phase mixing between the metastable cubic and hexagonal phases may severely influence the determination of the fundamental material parameters.

In this letter we report on the growth, the structural, and optical properties of *c*-InN epitaxial layers on *c*-GaN/3*C*-SiC hybride substrates. A decrease of hexagonal inclusions on the (111) facets with decreasing growth temperature was observed. Optical properties were derived by photoluminescence (PL) and spectroscopic ellipsometry measurements.

Cubic InN films were grown on top of a *c*-GaN buffer layer (600 nm) by rf-plasma assisted molecular beam epitaxy at different growth temperatures. The *c*-GaN buffer layer was deposited on a free standing 3*C*-SiC (001) substrate at a growth temperature of 720 °C. To reduce the thermal dissociation of In–N bonds the growth temperature was decreased for InN growth. The substrate temperature was varied in the range of 419–490 °C. We started the InN growth under In-rich conditions at an In-beam equivalent pressure of 6.8×10^{-8} mbar which was decreased to 3.1×10^{-8} mbar after 2 min of growth. The thicknesses of the InN layers were at least 130 nm and the growth was continuously monitored by reflection high energy electron diffraction (RHEED). Structural characterization was carried out by high resolution x-ray diffraction (HRXRD). Optical properties were obtained from room temperature spectroscopic ellipsometry measurements and photoluminescence measurements at 10 K using the 488 nm line of an Ar^+ laser. The luminescence signal was detected with an InAs photodiode with a cutoff wavelength of 3.6 μm.

HRXRD investigations were performed to determine the phase purity of our *c*-InN layers. All ω-2Θ scans confirmed the formation of the cubic phase of InN. Bragg peaks observed at 35.8°, 39.9°, and 41.3° correspond to *c*-InN (002), *c*-GaN (002), and 3*C*-SiC (002), respectively. No additional reflexion of *h*-InN grown in (0002) direction (at 31.4°) was detected. The full width at half maximum (FWHM) of the *c*-InN (002) rocking curve was 48 arc min. The lattice constant derived from the ω-2Θ scan is 5.01±0.01 Å, which is in good agreement with the value derived from the streak distance of the RHEED pattern and with values published by Bagayoko *et al.*[11] However, it is well known from *c*-GaN that hexagonal inclusions mainly grow on (111) facets and cannot be detected in ω-2Θ scans. Therefore reciprocal space maps (RSMs) of the GaN (002) Bragg reflex were measured. The RSM along the (-110) azimuth is shown in Fig. 1. The growth temperature of this InN sample was 419 °C. From the intensity ratio of the cubic (002) reflex and the hexagonal (10-11) reflex, we estimate 95% cubic phase in this InN layer, which is one of the best values reported for *c*-InN. Recently, some authors report on phase purities of 65% and 82% on *c*-InN.[12,13] Reciprocal space maps of the asymmetric GaN (-1-13) reflex show that the lattice of our *c*-InN layers is fully relaxed with respect to the *c*-GaN buffer.

In Fig. 2 we plot the ratio of the intensities of the *h*-(10-11) Bragg reflex and the *c*-(002) reflex versus the growth temperature of different InN layers. We observe a

[a]Electronic mail: li_jsch@physik.upb.de

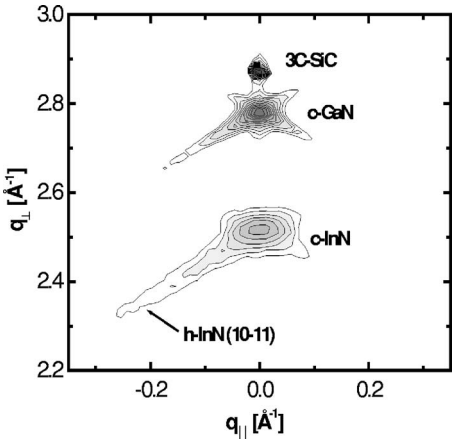

FIG. 1. Reciprocal space map of a *c*-InN layer. High intensity (002) Bragg reflexes of *c*-InN, *c*-GaN, and the 3*C*-SiC substrates are observed. Only a very weak (10-11) reflex from *h*-InN inclusions is measured yielding a content of hexagonal inclusion of about 5%.

strong decrease of hexagonal inclusions with decreasing growth temperature up to a minimum value of 5%. Our interpretation is that with decreasing growth temperature the sticking coefficient of In is increasing, resulting in a higher density of nuclei on the surface which can reduce the formation of (111) facets.

Figure 3 shows the low temperature PL spectrum of an InN layer grown at 419 °C. All *c*-InN films measured show a PL band around 0.69 eV with a FWHM of 170 meV. We suppose that the broadening of the luminescence is due to the fact that we have a degenerated semiconductor where the transition of the electrons from the conduction band can happen in a large energy range. The high density of dislocations ($\sim 10^{11}$ cm^{-2}) in our *c*-InN layer is responsible for the relatively weak intensity. The line shape of the luminescence which is also shown in Fig. 3 (full curve) was calculated using Eq. (1) of Ref. 14. As shown in Ref. 14, the low energy onset of the PL fitting curve defines the renormalized band gap $E_g(n)$, which approaches the band gap E_g at vanishing free carrier concentration $n=0$. We find a value of $E_g(n)$, which is close to 0.56 eV. Assuming a difference of about 50 meV between E_g and $E_g(n)$,[14] we get a low temperature band gap of *c*-InN close to 0.61 eV. If we take into account a temperature shift of about 50 meV (Ref. 15) between low

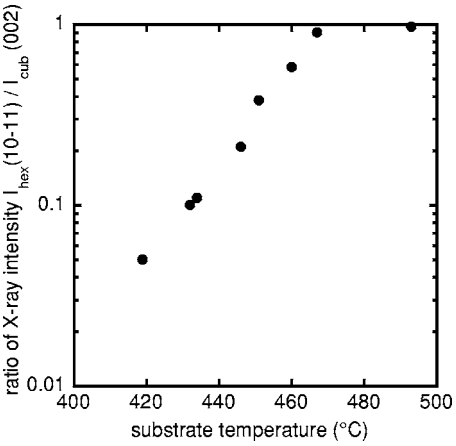

FIG. 2. Intensity of the (10-11) reflex of hexagonal inclusions over the intensity of the (002) Bragg reflex of cubic InN vs growth temperature of *c*-InN layers.

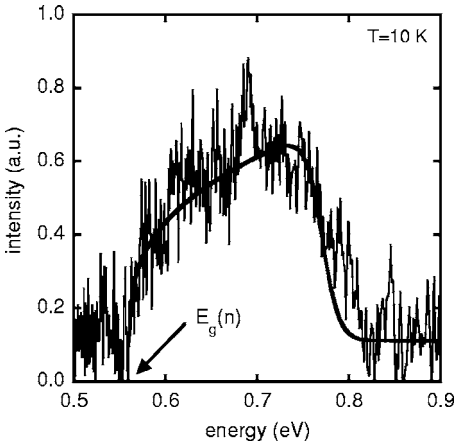

FIG. 3. Experimental and calculated photoluminescence spectra of a *c*-InN layer at 10 K. The position of $E_g(n)$ is indicated.

and room temperature the room temperature band gap of *c*-InN is about 0.56 eV.

The real (ε_1) and imaginary (ε_2) parts of complex dielectric function ($\bar{\varepsilon}$) for cubic InN were determined by spectroscopic ellipsometry at room temperature using the multilayer approach described in Ref. 16. No assumption was made concerning the spectral dependence of $\bar{\varepsilon}$ yielding parameter-free values for ε_1 and ε_2 at all photon energies. The results are shown in Fig. 4. The imaginary part is zero below 0.7 eV, it increases up to $\sim$1.3 eV and becomes nearly constant at higher photon energy. A similar behavior was previously found for *h*-InN (Ref. 17) and is typical for a degenerated semiconductor. Applying the line shape analysis for ε_2 as described in Ref. 17, the position of the Fermi energy is estimated with 0.93 eV for this sample. The maximum of ε_1 at 0.93 eV mirrors the shape of ε_2 which is expected due to the Kramers-Kronig relation between both parts of the dielectric function. We can use Eq. (1) to calculate the carrier concentration from the observed Burstein-Moss shift E_{BSM} of 0.37 eV,

$$E_{\mathrm{BMS}} = \Delta E_C + |\Delta E_V| = \frac{\hbar^2}{2}\left(\frac{m_e + m_h}{m_e m_h}\right)(3\pi^2 n)^{2/3}, \qquad (1)$$

where n is the free carrier concentration. The effective masses of electrons and holes in *c*-InN are $m_e=0.07m_0$ (Ref. 18) and $m_h=0.84m_0$,[2] respectively. Assuming a room tem-

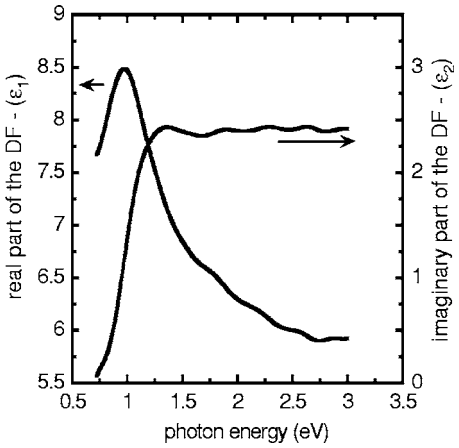

FIG. 4. Real and imaginary parts of the complex dielectric function of cubic InN. The Fermi energy lies about 0.93 eV above the valence band edge.

perature band-gap energy of *c*-InN of about 0.56 eV a carrier concentration of $n \sim 1.7 \times 10^{19}$ cm^{-3} is obtained.

In summary cubic InN layers were grown on *c*-GaN buffer layers at different growth temperatures. The phase purity of our *c*-InN layers increases with decreasing growth temperature. Cubic InN layers with only 5% hexagonal inclusions were grown at a substrate temperature of 419 °C. A minimum half width of the (002) XRD rocking curve of 48 arc min and a lattice constant of 5.01 ± 0.01 Å were measured. Low temperature (10 K) photoluminescence measurements reveal a *c*-InN band gap of about 0.61 eV. Spectroscopic ellipsometry measurements yield a Burstein shift of 370 meV and a respective carrier concentration of about 1.7×10^{19} cm^{-3}.

The authors would like to thank H. Nagasawa and M. Abe from HOYA Corporation, SiC Development Center, for supplying the 3*C*-SiC substrates.

[1]B. E. Fortz, S. K. O'Leary, M. S. Shur, and L. F. Eastman, J. Appl. Phys. **85**, 7727 (1999).
[2]S. K. Pugh, D. J. Dugdale, S. Brand, and R. A. Abram, Semicond. Sci. Technol. **14**, 23 (1999).
[3]C. Trager-Cowan, Phys. Status Solidi C **2**, 2240 (2005).
[4]V. Yu. Davydov, A. A. Klochikhin, R. P. Seisyan, V. V. Emtsev, S. V. Ivanov, F. Bechstedt, J. Furthmüller, H. Harima, A. V. Mudryi, J. Aderhold, O. Semchinova, and J. Graul, Phys. Status Solidi B **229**, R1 (2005).
[5]C. S. Gallinat, G. Koblmüller, J. S. Brown, S. Bernardis, and J. S. Speck, Appl. Phys. Lett. **89**, 032109 (2006).
[6]S. P. Fu, T. T. Chen, and Y. F. Chen, Semicond. Sci. Technol. **21**, 244 (2006).
[7]W. Walukiewicz, J. W. Ager III, K. M. Yu, Z. Liliental-Weber, J. Wu, S. X. Li, R. E. Jones, and J. D. Denlinger, J. Phys. D **39**, R83 (2006).
[8]F. Bechstedt, J. Furthmüller, M. Ferhat, L. K. Teles, L. M. R. Scolfaro, J. R. Leite, V. Yu. Davydov, O. Ambacher, and R. Goldhahn, Phys. Status Solidi A **195**, 628 (2003).
[9]D. J. As, in *Optoelectronic Properties of Semiconductor and Superlattices*, edited by M. O. Manasreh (Taylor & Francis, New York, 2003), Vol. 19, Chap. 9, pp. 323–450.
[10]D. J. As, S. Potthast, J. Schörmann, S. F. Li, K. Lischka, H. Nagasawa, and M. Abe, Mater. Sci. Forum **527–529**, 1489 (2006).
[11]D. Bagayoko, L. Franklin, and G. L. Zhao, J. Appl. Phys. **96**, 4297 (2004).
[12]K. Nishida, Y. Kitamura, Y. Hijikata, H. Yaguchi, and S. Yoshida, Phys. Status Solidi B **241**, 2839 (2004).
[13]T. Nakamura, K. Iida, R. Katayama, T. Yamamoto, and K. Onabe, Phys. Status Solidi B **243**, 1451 (2006).
[14]V. Y. Davydov, A. A. Klochikhin, V. V. Emtsev, D. A. Kurdykov, S. V. Ivanov, V. A. Vekshin, F. Bechstedt, J. Furthmüller, J. Aderhold, J. Graul, A. V. Mudryi, H. Harima, A. Hashimoto, A. Yamamoto, and E. E. Haller, Phys. Status Solidi B **234**, 787 (2002).
[15]W. Walukiewicz, Physica E (Amsterdam) **20**, 300 (2004).
[16]R. Goldhahn, J. Scheiner, S. Shokhovets, T. Frey, U. Köhler, D. J. As, and K. Lischka, Appl. Phys. Lett. **76**, 291 (2000).
[17]R. Goldhahn, P. Schley, A. T. Winzer, G. Gobsch, V. Cimalla, O. Ambacher, M. Rakel, C. Cobet, N. Esser, H. Lu, and W. J. Schaff, Phys. Status Solidi A **203**, 42 (2006).
[18]I. Vurgaftman and J. R. Meyer, J. Appl. Phys. **94**, 3675 (2003).